RESEARCH ARTICLE

BORNEO SCIENCE
THE JOURNAL OF SCIENCE & TECHNOLOGY

Journal homepage: https://jurcon.ums.edu.my/ojums/index.php/borneo-science

EFFECTS OF CO-ADSORBENT SILANE COUPLING AGENT STRUCTURE ON THE PERFORMANCE OF N719-BASED DYE-SENSITIZED SOLAR CELLS: AN EXPERIMENTAL AND DENSITY FUNCTIONAL THEORY INVESTIGATION

Cornellia Geoffrey[1], Edmund Engilip[1], Ivan Giggs Bin Florence[1], Jefany Joel Dapanis[1], Rachel Fran Mansa[2], Jedol Dayou[1], Alvie Lo Sin Voi*[1]

[1] Faculty of Science and Technology, Universiti Malaysia Sabah, Jalan UMS, 88400 Kota Kinabalu, Sabah, Malaysia.
[2] Faculty of Engineering and Technology, Universiti Malaysia Sabah, Jalan UMS, 88400 Kota Kinabalu, Sabah, Malaysia.

*** Correspondence:**
lv@ums.edu.my

Received: 08 May2026
Revised: 26 June 2026
Accepted: 26 June 2026
Published online: 26 June 2026

Doi : 10.51200/bsj.v47i1.6582

Keywords:
Dye-sensitized Solar Cells; Silane Coupling Agent; Co-adsorbant; Density Functional Theory.

ABSTRACT. *Charge recombination at the TiO_2–electrolyte interface remains a major limitation to the efficiency of dye-sensitized solar cells (DSSCs). In this work, the effect of silane coupling agents as co-adsorbents in N719-based DSSCs was systematically investigated. Eight silane derivatives with different molecular structures—TESF, 14BTEP, 13BTEP, B3TEP, TEVS, MPTS, IZPES, and BTEBP—were incorporated alongside the N719 dye, and their photovoltaic performance was compared with a control device prepared without silane. The control cell exhibited a power conversion efficiency (η) of 7.1%. Among the silane-modified devices, BTEBP achieved the highest efficiency of 7.4%, followed closely by IZPES at 7.3%, while 13BTEP and B3TEP showed reduced efficiencies of 6.7% and 6.8%. Density functional theory (DFT) calculations at the B3LYP/6-31G(d) level on isolated silane molecules provided molecular thickness (h) and chain size (d) descriptors. A clear structure–performance relationship emerged: an optimal silane thickness of ~8–13 Å combined with bulky chain geometry was most effective for TiO_2 surface passivation. These results demonstrate that silane co-adsorbent influence on DSSC performance strongly depends on molecular structure.*

INTRODUCTION

Dye-sensitized solar cells (DSSCs) are widely regarded as a promising third-generation photovoltaic technology due to their low fabrication cost, simple processing techniques, and good performance under diffuse and low-light conditions (O'Regan & Grätzel, 1991; Hagfeldt et al., 2010; Abdulsalami et al., 2026). Despite these advantages, the power conversion efficiency of DSSCs remains limited by interfacial charge recombination, particularly at the TiO_2/dye/electrolyte interface. Recombination between electrons injected into the TiO_2 conduction band and oxidized species in the electrolyte significantly reduces photocurrent density and overall device efficiency (Rühle et al., 2005; Zaine et al., 2020; Ashrafuzzaman et al., 2025; Arkan et al., 2024).

To address recombination losses, various interfacial engineering strategies have been developed, including surface passivation layers, surface doping, and the use of co-adsorbents. Co-adsorbents are typically small molecules introduced alongside sensitizing dyes to passivate uncovered TiO_2 surface sites, suppress electron–electrolyte recombination, and regulate dye adsorption to reduce aggregation (Liang et al., 2010; Gierszewski et al., 2019; Ren et al., 2022; Dissanayake et al., 2025). Surface passivation using organic, inorganic, or hybrid layers has been shown to prolong electron lifetime and improve open-circuit voltage in DSSCs (Park et al., 2012b; Tehare et al., 2018; Suresh et al., 2018).

Among the various surface modifiers investigated, silane-based compounds have attracted increasing attention due to their strong affinity for metal oxide surfaces and their ability to form stable Si–O–Ti bonds. Silane coupling agents can chemically anchor to TiO_2 surfaces, effectively passivating surface defects and limiting direct electrolyte contact with the semiconductor (Sewvandi et al., 2014). Experimental studies have demonstrated that silane modification of TiO_2 photoanodes can suppress charge recombination, enhance dye coverage, and improve device efficiency (Sewvandi et al., 2014; Neo & Ouyang, 2011; Dissanayake et al., 2025).

In addition to passivation, silane modification has been shown to influence dye organization and interfacial properties. Molecular-scale surface treatments can affect dye packing density, aggregation behavior, and interfacial energetics, thereby impacting short-circuit current density and fill factor (Rühle et al., 2005; Sobuś et al., 2018). The effectiveness of silanes as back-electron blocking agents has been suggested to depend on their molecular structure (Jung et al., 2014; Sewvandi et al., 2014). Despite these promising findings, systematic experimental investigations comparing different silane molecular structures on DSSC performance remain limited.

In this study, a series of silane derivatives are employed as co-adsorbents together with N719 dye on TiO_2 photoanodes. DFT calculations on isolated silane molecules provide molecular thickness (h) and chain size (d) descriptors correlated with experimental performance to establish structure–performance relationships (Arkan et al., 2024). This work aims to provide experimental and computational insight into the role of silane chemistry in interfacial passivation and to establish molecular design principles for optimizing dye-sensitized solar cells.

MATERIALS AND METHODS

Materials

All chemicals were used as received. Anatase-phase TiO_2 paste (Ti-Nanoxide T/SP, ~20 nm), N719 dye (Ruthenizer 535-bisTBA), iodide/triiodide electrolyte (Iodolyte Z-50), platinum paste (Platisol T/SP), and fluorine-doped tin oxide (FTO) glass substrates (TCO Glass-22, 8–12 Ω cm^{-1}, 2.2 mm thickness) were purchased from Solaronix. Surlyn® thermoplastic film (25 μm, Meltonix 1170-25) was used as spacer and sealant. Silane coupling agents were obtained from Sigma-Aldrich (≥97%): 3-(triethoxysilyl)furan (TESF), 1,4-bis(triethoxysilyl)benzene (14BTEP), 1,3-bis(triethoxysilyl)benzene (13BTEP), bis[3-(triethoxysilyl)propyl]tetrasulfide (B3TEP), triethoxyvinylsilane (TEVS), 3-mercaptopropyltriethoxysilane (MPTS), triethoxy-3-(2-imidazolin-1-yl)propylsilane (IZPES), and 4,4′-bis(triethoxysilyl)-1,1′-biphenyl (BTEBP).

DSSCs Fabrication

TiO_2 photoanodes were prepared on pre-cleaned FTO glass substrates. The nanoporous TiO_2 electrode consisted of two layers deposited by the doctor-blade method: a first layer of 20 nm TiO_2 nanoparticles (Ti-Nanoxide T/SP) and a second scattering layer of 100 nm particles (Ti-Nanoxide R/SP). After printing the first layer, the glass was sintered at 300 °C for 10 min; following deposition of the second layer, the electrode was sintered at 500 °C for 1 h to crystallize both layers (total film thickness ~10–12 μm).

N719 dye was dissolved in anhydrous acetonitrile to a concentration of 0.3 mM and magnetically stirred for 30 min at room temperature. Dye solutions were stored in aluminium foil-covered containers below 25 °C. Eight silane stock solutions were prepared by dissolving each silane in anhydrous acetonitrile at mass concentrations equivalent to the N719 dye solution. Equal volumes of dye and silane solutions were combined (1:1, v:v) under gentle stirring, maintaining a constant N719 concentration of 0.3 mM and a dye-to-silane weight ratio of 1:1.

Interfacial modification was carried out via a sequential protocol (Sewvandi et al., 2014). TiO_2 electrodes were first immersed in the control dye solution for 24 h at room temperature, then transferred to the respective dye–silane pre-mixed solutions for 2 h. Electrodes were rinsed with anhydrous ethanol and dried under inert atmosphere. Platinum counter electrodes were prepared by doctor-blading Pt paste onto FTO glass and sintering at 400 °C for 15 min. Cells were assembled using a 25 µm Surlyn spacer. The electrolyte (0.5 M 1-methyl-3-propylimidazolium iodide, 0.05 M I_2, 0.1 M TBP in acetonitrile) was introduced by vacuum backfilling. Assembled cells were stored in the dark for 12 h prior to measurement.

Photovoltaic Performance

Current–voltage (J–V) measurements were performed using a Class AAA solar simulator (YOHA YHCT-AAA) under simulated AM 1.5G illumination (100 mW cm^{-2}). Spectral mismatch was below 2% and spatial uniformity exceeded 95% over a 2 × 2 cm^2 active area. Voltage scans were conducted from −0.1 to 0.8 V with a step size of 0.01 V and a delay time of 50 ms at 25 ± 1 °C and 40 ± 5% relative humidity. Light intensity was calibrated using an NREL-certified silicon reference cell. Each device was measured three times; reported parameters (Jsc, Voc, FF, η) represent averaged values with standard deviations below 3%.

Computational Method

DFT calculations were performed using Gaussian 09 at the B3LYP/6-31G(d) level (Arkan et al., 2024) on isolated silane molecules in the vacuo. Each silane molecule was subjected to full geometry optimization without symmetry constraints. Two molecular descriptors were computed from the optimized ground-state geometries: (i) molecular thickness h (Å), the maximum vertical extent of the silane molecule, representing the effective length of the passivation layer when adsorbed on TiO_2; and (ii) chain size d (Å), the maximum lateral spatial extent of the silane molecule, representing molecular bulkiness and the surface area potentially shielded by each silane upon TiO_2 adsorption.

RESULTS AND DISCUSSION

DSSCs performance

The prepared selected DSSCs is shown in Figure 1. The J–V characteristics are shown in Figure 3 and the corresponding parameters are compiled in Table 1. The control DSSC (N719, without silane) showed Jsc = 17.3 mA cm^{-2}, Voc = 0.73 V, FF = 0.56, and η = 7.1%.

Three devices demonstrated enhanced PCE compared to the control. BTEBP achieved the highest PCE of 7.4% (~4.2% relative improvement), attributable to increased FF (0.58) and slightly higher Jsc (17.4 mA cm^{-2}). IZPES exhibited the second-highest PCE of 7.3%, driven by the highest Jsc among all silanes (17.7 mA cm^{-2}) and improved FF of 0.58. The 14BTEP sample also reached 7.3% efficiency, matching IZPES but with higher Voc (0.73 V). These results are consistent with recent findings that appropriately chosen co-adsorbents can substantially enhance DSSC performance (Dissanayake et al., 2025).

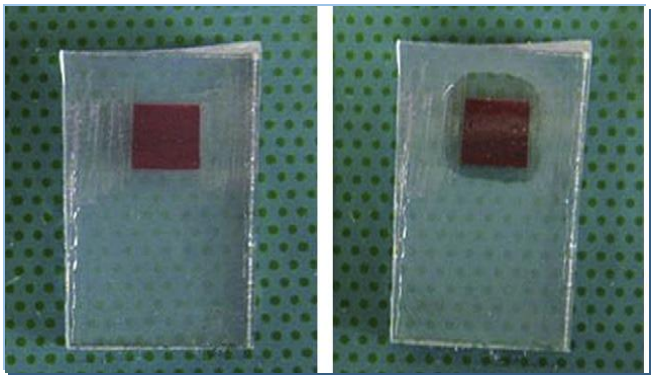

Figure 1. Fabricated silane co-adsorbs N719 base DSSCs using doctor blade method.

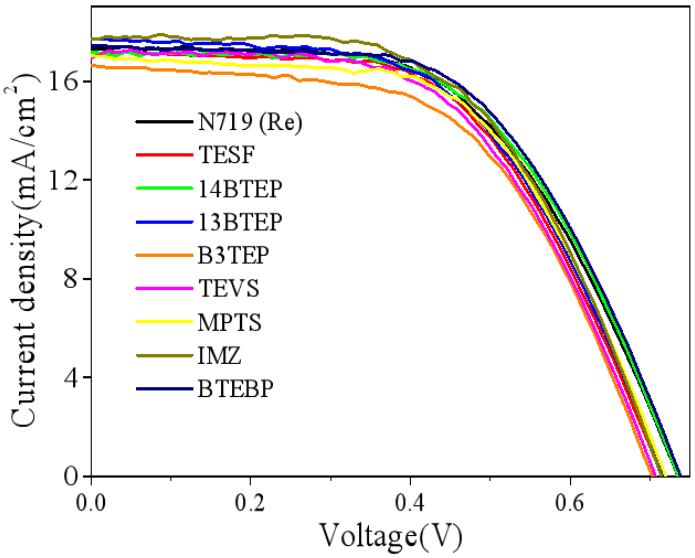

Figure 2. J–V characteristics of N719 base DSSCs incorporating different silane co-adsorbents under AM 1.5G illumination (100 mW cm^{-2}).

Table 1. Photovoltaic parameters of N719 base DSSCs with different silane co-adsorbents under AM 1.5G illumination (100 mW cm^{-2}).

Sample	Jsc (mA cm^{-2})	Voc (V)	FF	η (%)
N719 (control)	17.3	0.73	0.56	7.1
TESF	17.2	0.72	0.57	7.0
14BTEP	17.2	0.73	0.56	7.3
13BTEP	16.6	0.71	0.57	6.7
B3TEP	17.0	0.71	0.56	6.8
TEVS	17.4	0.73	0.58	7.4
MPTS	17.3	0.73	0.57	7.1
IZPES	17.7	0.71	0.58	7.3
BTEBP	17.4	0.74	0.58	7.4

Devices with 13BTEP and B3TEP underperformed relative to the reference cells. The 13BTEP-modified device recorded the lowest PCE of 6.7% (Jsc = 16.6 mA cm^{-2}, Voc = 0.71 V). B3TEP yielded 6.8% (Jsc = 17.0 mA cm^{-2}, Voc = 0.71 V). The remaining silanes (TESF, MPTS) produced parameters comparable to the control.

A notable observation is that all silane-treated cells matched or exceeded the control FF of 0.56, with BTEBP, IZPES, and TEVS reaching 0.58. This universal FF enhancement is attributed to Si–O–Si siloxane network formation within the TiO_2 film during co-adsorption, which bridges adjacent nanoparticles and improves inter-particle electronic connectivity (Park et al., 2012a). The variation in Voc was relatively modest across all devices (0.70–0.74 V), consistent with a physical surface blocking mechanism.

Silane Structure–Performance Correlations

Optimized geometry of the silane molecule obtained from the DFT calculations at the B3LYP/6-31G(d) are shown in Figure provided molecular thickness (h) and chain size (d) descriptors. Table 2 summarizes the computed h and d values alongside experimental efficiency.

Table 2. DFT-computed molecular thickness (h) and chain size (d) at the B3LYP/6-31G(d) level on isolated silane molecules, with corresponding experimental efficiency.

Silane	h (Å)	d (Å)	η (%)
N719 (control)	—	—	7.1
TESF	5.0	3.6	7.0
14BTEP	9.3	8.8	7.3
13BTEP	9.3	8.8	6.7
B3TEP	18.0	9.2	6.8
TEVS	3.3	1.4	7.4
MPTS	5.8	1.0	7.1
IZPES	7.8	3.4	7.3
BTEBP	13.3	9.3	7.4

The combined experimental and DFT dataset reveals clear structure–performance relationships governing silane effectiveness as co-adsorbents in N719-based DSSCs. Molecular thickness (h) — optimal range ~8–13 Å. Silanes with thickness in this range — 14BTEP (h = 9.3 Å, η = 7.3%), IZPES (h = 7.8 Å, η = 7.3%), and BTEBP (h = 13.3 Å, η = 7.4%) — all outperformed the control device. This thickness range corresponds approximately to the estimated thickness of the N719 sensitizer layer (~12 Å), suggesting that effective passivation requires the silane to be of comparable height to the dye molecules. Silanes that are substantially shorter, such as TESF (h = 5.0 Å) and TEVS (h = 3.3 Å), provide insufficient physical blocking. Conversely, B3TEP (h = 18.0 Å, η = 6.8%) may form a barrier so thick that it hinders I^- access for dye regeneration.

The shielding effect provided by the modifier is heavily influenced by its chain size. Bulkier geometries are inherently better suited to passivate the surface; accordingly, the highest-performing molecules, BTEBP (d = 9.3 Å) and 14BTEP (d = 8.8 Å), feature the largest overall chain sizes. The necessity of this steric bulk is further proven by MPTS; with the smallest chain size evaluated (d = 1.0 Å), it demonstrated a baseline performance on par with the control, reinforcing that nominal chain sizes lack the capacity for effective surface shielding (Dissanayake et al., 2025).

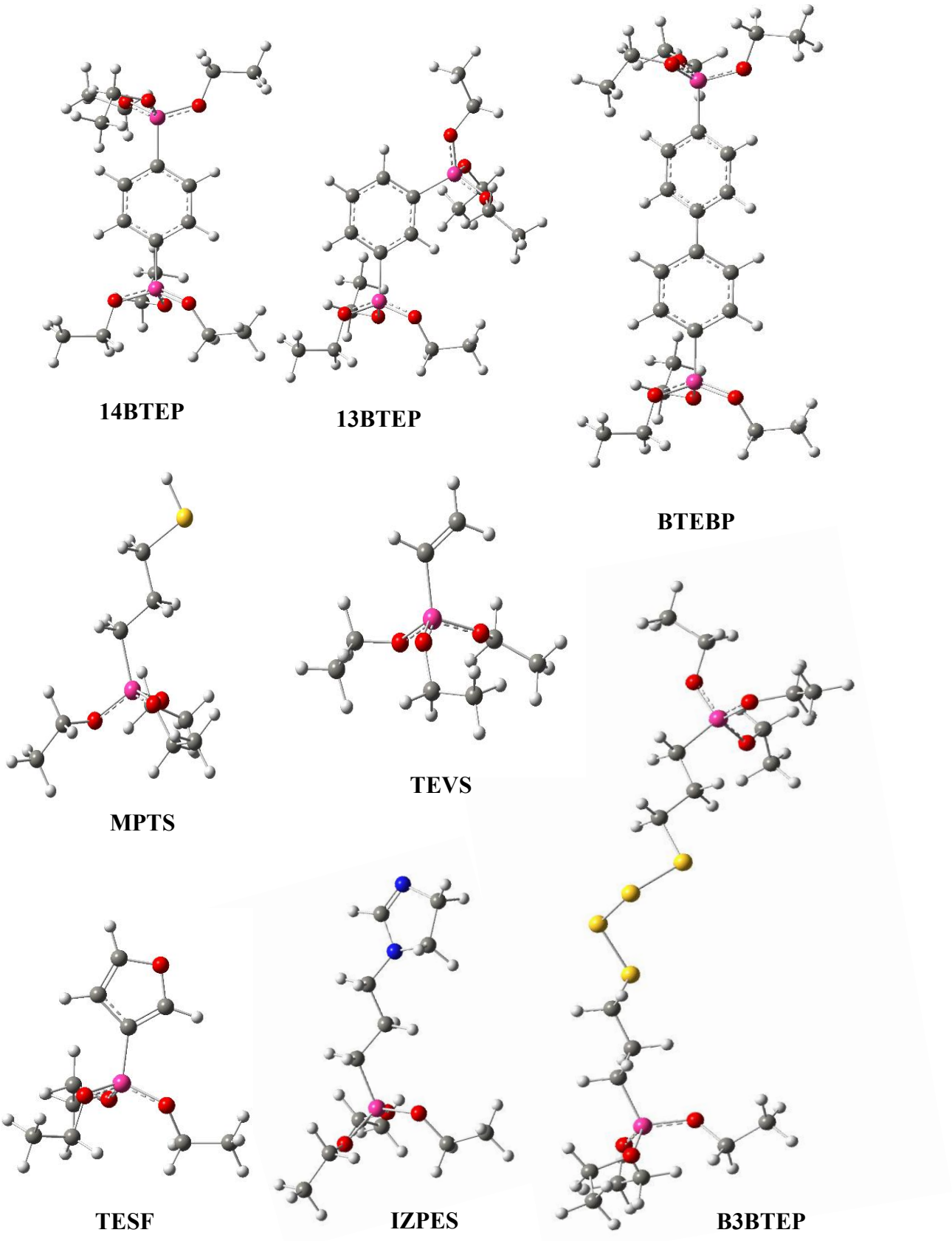

Figure 3. Optimize geometry of Silanes Molecule using B3LYP/6-31G(d) level of theory.

The case of TEVS (h = 3.3 Å, d = 1.4 Å) which is the smallest silane investigated yet achieves the highest efficiency (7.4%) alongside BTEBP. Under the sequential fabrication protocol, the compact TEVS molecules may preferentially adsorb into narrow interstitial spaces between pre-adsorbed dye molecules "interstitial filling" enabling targeted passivation of the most critically exposed TiO_2 sites. The high FF (0.58) supports efficient electron transport via siloxane networks (Park et al., 2012a).

CONCLUSION

The influence of silane co-adsorbents with different molecular structures on the photovoltaic performance of N719-based DSSCs was systematically investigated through combined experimental measurements and DFT calculations on isolated silane molecules. Among the eight silane derivatives tested, BTEBP and TEVS achieved the highest PCE of 7.4%, while IZPES and 14BTEP reached 7.3%, all exceeding the control device (7.1%). In contrast, 13BTEP (6.7%) and B3TEP (6.8%) reduced device performance.

DFT calculations on isolated silane molecules identified an optimal molecular thickness of approximately 8–13 Å corresponding to the N719 sensitizer layer thickness. Silanes that are too short provided insufficient blocking, while those excessively long hindered dye regeneration. Bulkier chain geometries enhanced surface shielding efficiency. All silane-treated devices exhibited fill factors equal to or higher than the control, attributed to improved inter-particle connectivity via Si–O–Si siloxane network formation. Molecular orientation governed by substitution pattern was shown to be as important as gross molecular dimensions.

These findings demonstrate that silane co-adsorbent performance strongly depends on molecular structure. The structure–performance relationships established herein provide design guidelines for rational selection and computational screening of silane co-adsorbents for DSSCs.

ACKNOWLEDGEMENT

The author would like to thank Malaysian Ministry of Higher Education for the financial support to the research through Fundamental Research Grant Scheme [FRG0593-1/2022].

REFERENCES

Abdulsalami, I. O., Omobhude, I. A., Abdulsalami, B. A., Younas, M., Semire, B., & Bello, I. A. (2026). Dye-sensitized solar cells: A systematic review of progress, challenges, and future perspectives. Discover Chemistry, 3, 87.

Arkan, F., Pakravesh, F., Barati Darband, F., Sabagh, S., & Izadyar, M. (2024). Recent progress toward high-performance dye-sensitized solar cells: A review. Journal of the Iranian Chemical Society, 21, 577–638.

Ashrafuzzaman, M., Ismail, M., Ali, A. K. M., Bhargava, S. K., Alam, M. K., & Anower, M. S. (2025). Impact of TiO_2 compact layer on the performance of dye-sensitized solar cells. Journal of Power Sources, 638, 236636.

Dissanayake, M. A. K. L., Sandunika, P. U., Senadeera, G. K. R., Kumari, J. M. K. W., Hettiarachchi, M. S. H., Subasinghe, J. L., Karunaratne, A. K., & Sandamali, W. I. (2025). Exploring linoleic acid as a novel co-adsorbent to enhance dye-sensitized solar cell efficiency through surface engineering of TiO_2 at the photoanode/electrolyte interface. Journal of Applied Electrochemistry, 55, 2947–2964.

Gierszewski, M., Falkowski, M., Sobuś, J., Stolarski, M., Popenda, L., Lijewski, S., Wicher, B., Burdzinski, G., Karolczak, J., Jurga, S., Graczyk, A., Marszalek, T., Zakeeruddin, S. M., Grätzel,

M., & Ziolek, M. (2019). Porphyrin-based symmetrical and unsymmetrical donor–acceptor dyes for DSSCs: The role of anchoring groups on photovoltaic performance. ACS Applied Materials & Interfaces, 11(3), 240–252.

Hagfeldt, A., Boschloo, G., Sun, L., Kloo, L., & Pettersson, H. (2010). Dye-sensitized solar cells. Chemical Reviews, 110(11), 6595–6663.

Jung, Y. S., Yoo, Y., Park, J. H., & Kim, H. K. (2014). Silane coupling agents for improving the photovoltaic performance of dye-sensitized solar cells. Bulletin of the Korean Chemical Society, 35(2), 415–420.

Liang, M., Zhong, X., & Ge, Z. (2010). Effect of co-adsorbents on TiO_2 interface and photovoltaic performance of dye-sensitized solar cells. Journal of Physical Chemistry C, 114(24), 10993–10998.

Neo, C. Y., & Ouyang, J. (2011). Functionalized carbon nanotubes with covalently attached silane for dye-sensitized solar cells. Journal of Power Sources, 196(23), 10538–10542.

O'Regan, B., & Grätzel, M. (1991). A low-cost, high-efficiency solar cell based on dye-sensitized colloidal TiO_2 films. Nature, 353(6346), 737–740.

Park, J. T., Prosser, J. H., Ahn, D. J., Kim, J. H., & Lee, D. (2012a). Enhancing the performance of solid-state dye-sensitized solar cells using a silane-based interfacial layer with controlled pore morphology. Electrochimica Acta, 59, 32–38.

Park, J. T., Chi, W. S., Roh, D. K., Ahn, S. H., & Kim, J. H. (2012b). Enhanced performance of dye-sensitized solar cells using silane-modified TiO_2 electrodes. Journal of Power Sources, 216, 36–41.

Ren, Y., Cao, Y., Zhang, D., Zakeeruddin, S. M., Hagfeldt, A., Wang, P., & Grätzel, M. (2022). A blue photosensitizer realizing efficient and stable green solar cells via color tuning by electrolyte. Nature, 613(7942), 60–65.

Rühle, S., Greenshtein, M., Chen, S. G., Merson, A., Pizem, H., Sukenik, C. S., Cahen, D., & Zaban, A. (2005). Molecular adjustment of the electronic properties of nanoporous electrodes in dye-sensitized solar cells. Journal of Physical Chemistry B, 109(40), 18907–18913.

Sewvandi, G. A., Tao, Z., Kusunose, T., Tanaka, Y., Nakanishi, S., & Feng, Q. (2014). Modification of TiO_2 electrode with organic silane interposed layer for high-performance of dye-sensitized solar cells. ACS Applied Materials & Interfaces, 6(8), 5818–5826.

Sobuś, J., Kubicki, J., Burdziński, G., & Ziółek, M. (2018). Carboxyl and amino groups in the structure of dye-sensitized solar cells: A femtosecond to nanosecond study of electron injection dynamics. Angewandte Chemie International Edition, 57(5), 1307–1311.

Suresh, R., Pandiaraj, K., Sankaralingam, M., & Giribabu, L. (2018). Graphene–TiO_2 composite photoanode for dye-sensitized solar cells. Electrochimica Acta, 289, 591–598.

Tehare, K. K., Bhande, S. S., Mutkule, S. U., Stadler, F. J., Ao, J. P., Mane, R. S., & Liu, X. (2018). Low-temperature chemical synthesis of ruthenium oxide and its TiO_2 based dye-sensitized solar cells. Materials Research Bulletin, 97, 351–360.

Zaine, S. N. A., Mohamed, N. M., Khatani, M., & Shadid, A. A. (2020). Nanoparticle size effects on TiO_2-based dye-sensitized solar cells. Coatings, 10(3), 284.